

## Hydrogen cyanide in comet C/1996 B2 Hyakutake

Karen Magee-Sauer

Department of Chemistry and Physics, Rowan University, Glassboro, New Jersey, USA

Michael J. Mumma

Laboratory for Extraterrestrial Physics, NASA Goddard Space Flight Center, Greenbelt, Maryland, USA

Michael A. DiSanti and Neil Dello Russo

Department of Physics, Catholic University of America, Washington, D. C., USA

Laboratory for Extraterrestrial Physics, NASA Goddard Space Flight Center, Greenbelt, Maryland, USA

Received 12 February 2002; revised 21 May 2002; accepted 29 May 2002; published 5 November 2002.

[1] Spectral emission from HCN in C/1996 B2 Hyakutake was detected on UT 1996 March 24.4 ( $r_h = 1.06$  AU,  $\Delta = 0.106$  AU), using the CSHELL infrared spectrometer at the NASA Infrared Telescope Facility. A Boltzmann analysis of eight ro-vibrational lines in the  $\nu_3$  band returned a rotational temperature ( $83 \pm 9$  K) for a region centered on the nucleus. The global HCN production rate was  $(4.50 \pm 0.81) \times 10^{26}$  molecules  $s^{-1}$ . The HCN abundance relative to water is then  $(0.18 \pm 0.04)\%$ , based on direct measurements of  $H_2O$  made on the same night with the same instrument and reduced with the same data processing algorithms. The measured spatial distribution for HCN is consistent with its release at the nucleus; no significant contribution from a distributed source is required within  $\sim 600$  km of the nucleus. We use these data to obtain insights regarding the origin of HCN in this comet. *INDEX TERMS:* 6210 Planetology: Solar System Objects: Comets; 6008 Planetology: Comets and Small Bodies: Composition; 6005 Planetology: Comets and Small Bodies: Atmospheres—composition and chemistry; *KEYWORDS:* Comets, infrared, spectroscopy, HCN, Hyakutake, hydrogen cyanide

**Citation:** Magee-Sauer, K., M. J. Mumma, M. A. DiSanti, and Neil Dello Russo, Hydrogen cyanide in comet C/1996 B2 Hyakutake, *J. Geophys. Res.*, 107(E11), 5096, doi:10.1029/2002JE001863, 2002.

### 1. Introduction

[2] Infrared spectroscopy has been a successful tool in measuring the abundances of natal ices in comets since the detection of water in comet Halley from the Kuiper Airborne Observatory [Mumma *et al.*, 1986; Weaver *et al.*, 1986]. Early applications of this approach from ground based observatories provided detections of cometary  $CH_3OH$  and CO [Hoban *et al.*, 1991; DiSanti *et al.*, 1992a] and sensitive upper limits to  $CH_4$  and OCS [Brooke *et al.*, 1991; DiSanti *et al.*, 1992b].

[3] In 1992, the first of the next-generation infrared instruments was commissioned at the NASA Infrared Telescope Facility (IRTF) atop Mauna Kea, Hawaii. CSHELL (the Cryogenic Echelle Spectrometer) was the first infrared spectrometer to combine high spectral resolving power with 2-D detector arrays optimized for the 1–5  $\mu m$  spectral region [Tokunaga *et al.*, 1990; Greene *et al.*, 1993]. With it, water was soon detected in two comets, confirming and extending the importance of ground-based infrared spectroscopy for studies of cometary composition [Mumma *et al.*, 1995a, 1995b]. Detection of the dominant parent volatile set

the stage for exploitation of this approach with the next bright comet.

[4] The first optimum cometary target for the CSHELL instrument appeared soon thereafter. Comet Hyakutake was discovered January 30, 1996 by Japanese amateur astronomer Yuji Hyakutake. Hyakutake was neither a big comet ( $\sim 3$  km in diameter [Harmon *et al.*, 1997]), nor did it have unusually large gas or dust production rates [Dello Russo *et al.*, 2002; Schleicher *et al.*, 1998; Biver *et al.*, 1999a]. However, owing to its close approach to Earth ( $\Delta = 0.1$  AU), it was the brightest comet to be seen from earth in  $\sim 20$  years.

[5] Abundance measurements and spatial characteristics were attained for numerous volatile species in comet Hyakutake (and in later comets) using CSHELL ( $H_2O$ , CO,  $CH_3OH$ ,  $CH_4$ ,  $C_2H_6$ ,  $C_2H_2$ , HCN, OCS,  $NH_3$ ,  $NH_2$ , OH,  $H_2CO$ , and other unidentified emissions) [Brooke *et al.*, 1996; Mumma *et al.*, 1996a, 1996b; Dello Russo *et al.*, 1998, 2000, 2001, 2002; DiSanti *et al.*, 1999, 2001; Magee-Sauer *et al.*, 1999; Weaver *et al.*, 1999]. Moreover, long slit spectra of Hyakutake obtained with CSHELL provided (for the first time) a means of determining the spatial distribution of the emission, permitting discrimination between material released from the nucleus (native ices) and that released in the coma (distributed sources).

[6] In this paper we report spectroscopic observations of the  $\nu_3$  ro-vibrational band of HCN in C/1996 B2 Hyakutake

**Table 1.** HCN Production Rate and Relative Abundance

Comet	Date, UT	$r_h$ , AU	$\Delta$ , AU	Lines Observed	$T_{\text{rot}}^a$ , K	$\beta$ , %	$Q(\text{HCN})$ , $10^{27}$ mol s $^{-1}$	$Q(\text{HCN})/$ $Q(\text{H}_2\text{O})$ , %
Hyakutake	1996 Mar 24.4	1.06	0.106	P2, P3, P5, P6, R1, R2 <sup>b</sup> , R3, R6, R8	$83 \pm 9$	42	$(0.45 \pm 0.08)$	$(0.18 \pm 0.04)$
Hale-Bopp <sup>c</sup>	1997 Feb 24.0	1.11	1.57	P2, P3, P4, P6, P7	120	25	$(23.9 \pm 6.0)$	$(0.27 \pm 0.04)$
	1997 Apr 6.10	0.92	1.40	P2, P3, R6	120	12	$(56.2 \pm 12.9)$	$(0.53 \pm 0.07)$
	1997 Apr 29.9	1.05	1.75	P2, P3, P4, P7, P8, P11, R6, R7	$122 \pm 8$	36	$(30.9 \pm 1.8)$	$(0.46 \pm 0.03)$
	1997 May 1.0	1.09	1.77	P3, P4, P5, P7	120	22	$(28.0 \pm 7.4)$	$(0.38 \pm 0.05)$
Lee <sup>d</sup>	1999 Aug 21.6	1.09	1.35	P2, P3, P4, P6, P7, P8, P9, R0, R1, R2, R3, R5, R6	$72 \pm 8$	63	$(0.29 \pm 0.02)$	$(0.23 \pm 0.02)$

<sup>a</sup> The rotational temperature for comets Lee and Hyakutake was for a region centered within a nucleus-centered box ( $1'' \times 1''$ ), for Hale-Bopp for a region extending  $2'' - 10''$  from the comet nucleus.

<sup>b</sup> The R2 line was not included in temperature, spatial profile, or production rate measurements since the line is blended with an emission identified as the 101-001  $3_{13}-4_{22}$  water line.

<sup>c</sup> Magee-Sauer et al. [1999].

<sup>d</sup> Mumma et al. [2001].

at infrared wavelengths near  $3.0 \mu\text{m}$ . From them, we obtain the rotational temperature of HCN, its absolute production rate, and its spatial distribution in the coma. We measured  $\text{H}_2\text{O}$  on the same night with CSHELL [Dello Russo et al., 2002], so we also obtain the abundance of HCN relative to water. We use these data to obtain insights regarding the origin of HCN in this comet.

## 2. Background

[7] HCN is a known component in cometary comae and is thought to be present as a native ice in the cometary nucleus where it could exist in both monomeric and polymeric forms. The abundance of HCN relative to other nitrogen bearing species (e.g.,  $\text{NH}_3$ ,  $\text{N}_2$ ) can indicate the temperature of formation and the kind and degree of processing experienced by precometary material, whether in the natal cloud or in the solar nebula [Mumma et al., 1993].

[8] HCN emits radiation in millimeter and infrared regions via rotational and ro-vibrational transitions, respectively. A detection of cometary HCN was first claimed at millimeter wavelengths in comet Kohoutek 1973 XII [Huebner et al., 1974] and a secure detection was obtained in comet 1P/Halley [Schloerb et al., 1986]. Measurements at millimeter wavelengths were obtained for numerous comets thereafter (see discussion by Magee-Sauer et al. [1999, and references therein]). With the high spectral dispersion and improved array detectors featured by the CSHELL instrument, HCN was first observed in the infrared in comet Hyakutake [Mumma et al., 1996a; Brooke et al., 1996].

## 3. Observations and Analysis

[9] Observations were acquired on UT March 24.4 1996 at the NASA IRTF under telescope time assigned for a ‘‘Target of Opportunity.’’ The geocentric distance of the comet was 0.106 AU and the heliocentric distance was 1.06 AU (Table 1).

[10] CSHELL incorporates a  $256 \times 256$  InSb array detector ( $0.2''$  pixels) with a long slit. We used the 5-pixel wide slit ( $1'' \times 30''$ ) (oriented east-west), corresponding to spatial dimensions  $77 \text{ km} \times 2300 \text{ km}$  at the comet on this

date. The spectral resolving power ( $\lambda/\Delta\lambda \sim 2 \times 10^4$ ) was sufficient to resolve individual cometary emission lines, and the high spatial resolution permitted measurements of the distribution of species within the inner coma. (Hyakutake was the first comet whose spectral lines were bright enough to permit measurement of their spatial profiles about the nucleus.) Absolute flux calibration was achieved through a comparison with the spectra of flux-standard stars. Our observing techniques and data reduction processes are described elsewhere [Dello Russo et al., 1998, 2000, 2001; DiSanti et al., 1999, 2001; Magee-Sauer et al., 1999].

[11] In order to obtain a good measure of the HCN rotational temperature, we sampled lines that spanned a wide range in rotational energy. Four separate grating settings were used, and the total time on source was 240 seconds for each setting. Spectra of the detected lines appear in Figures 1a–1d, and a synopsis is given in Table 1. A typical processed data frame results in a 2-D spectral-spatial display of cometary molecular and continuum emission. We extracted spectra for one arcsecond square ( $5 \text{ pixel} \times 5 \text{ pixel}$ , or  $77 \text{ km} \times 77 \text{ km}$ ) regions centered on the comet nucleus. Nine ro-vibrational lines of HCN appear in our flux calibrated spectra of comet Hyakutake (Figures 1a–1d). Emission lines of other species are also detected, including  $\text{C}_2\text{H}_2$ ,  $\text{NH}_2$ ,  $\text{NH}_3$ , OH (both prompt and resonant fluorescent),  $\text{H}_2\text{O}$  (hot-band emission), and other unidentified emissions. Results and analysis of these emissions will be presented in future papers.

## 4. Results

### 4.1. Rotational Temperature

[12] HCN emission lines were detected with high signal-to-noise ratio over a region  $\sim \pm 200 \text{ km}$  about the nucleus of Hyakutake. They represent a fraction of the total  $\nu_3$  intensity that depends on the rotational distribution, so it is necessary to determine the rotational temperature before calculating a total production rate. Since our long-slit spectra sample some lines of sight that include regions very close to the nucleus, we examined whether we needed to consider optical depth effects in our calculations. DiSanti et al. [2001] presented a general formalism to examine optical

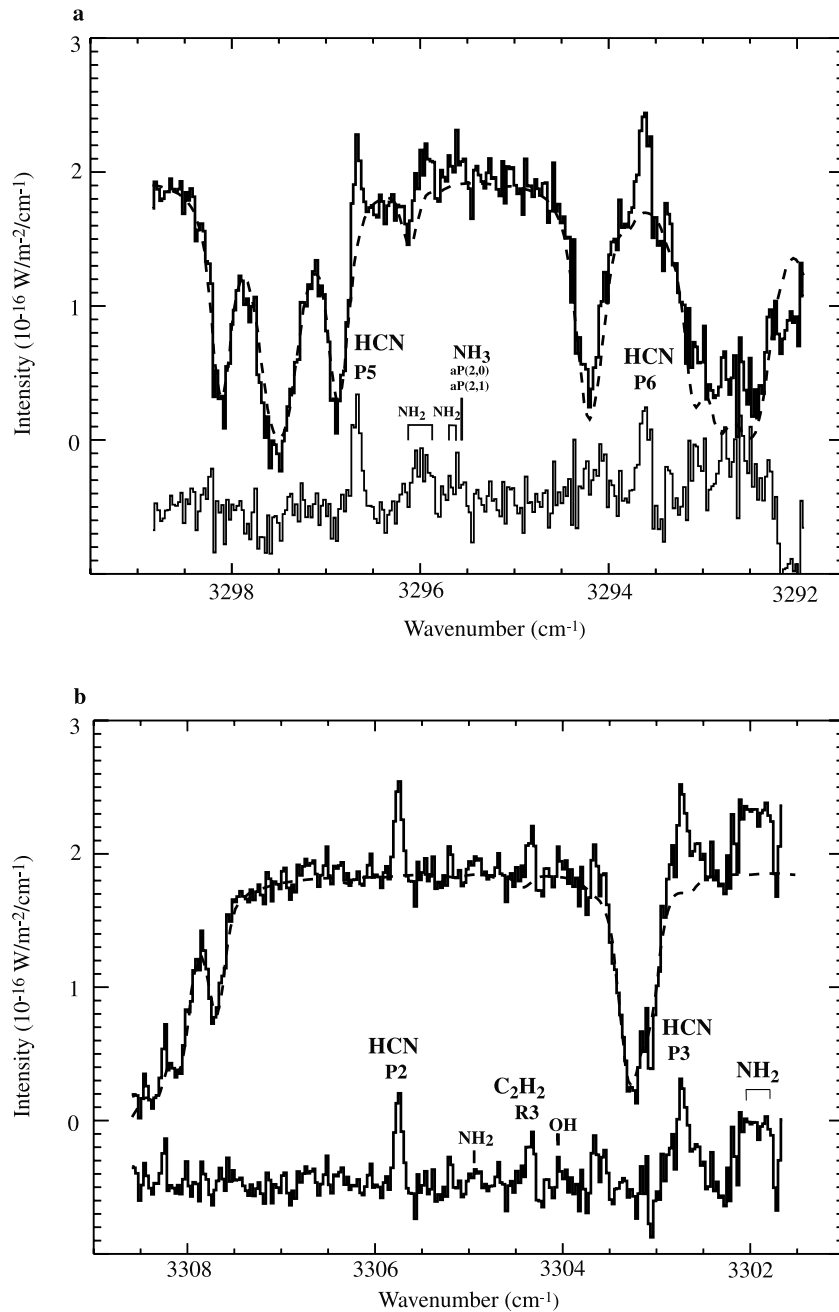


**Figure 1.** Flux-calibrated spectra of Comet Hyakutake for four grating settings obtained on UT 1996 March 24.4. Each figure shows cometary continuum and molecular emission lines (solid curve), normalized atmospheric transmittance spectrum (dashed line), and their difference. As seen in Figures 1a–1d, the 3- $\mu\text{m}$  region is rich in cometary molecular line emissions. HCN, C<sub>2</sub>H<sub>2</sub>, OH, NH<sub>2</sub>, H<sub>2</sub>O, and unidentified species were detected. The HCN R2 line is blended with a relatively strong H<sub>2</sub>O hot-band transition [101-001] (3<sub>12</sub>–4<sub>22</sub>).

depth effects in the analysis of CO production. They define a critical radius ( $R_c$ ), the distance from the nucleus at which the optical depth of a given line reaches unity at line center ( $\tau = 1$ ) along a radius vector from the Sun to  $R_c$ . We calculate this parameter for the HCN lines used in this analysis. In all cases,  $R_c$  is less than 1 km (the maximum value is  $\sim 0.8$  km for the R3 line; see Table 2). Therefore, optical depth corrections are negligible for HCN lines used in this analysis.

[13] The rotational temperature is obtained from the intensity of individual ro-vibrational transitions via Boltzmann analysis [Herzberg, 1950, p. 126; DiSanti *et al.*, 1999, 2001; Magee-Sauer *et al.*, 1999]. Eight of the nine ro-vibrational HCN lines observed in Hyakutake were used (Table 1). (The R2 line was excluded since it is blended with a relatively strong H<sub>2</sub>O hot-band transition 101-001 (3<sub>12</sub>–4<sub>22</sub>)). The population is seen to be consistent with a single temperature (Figure 2).

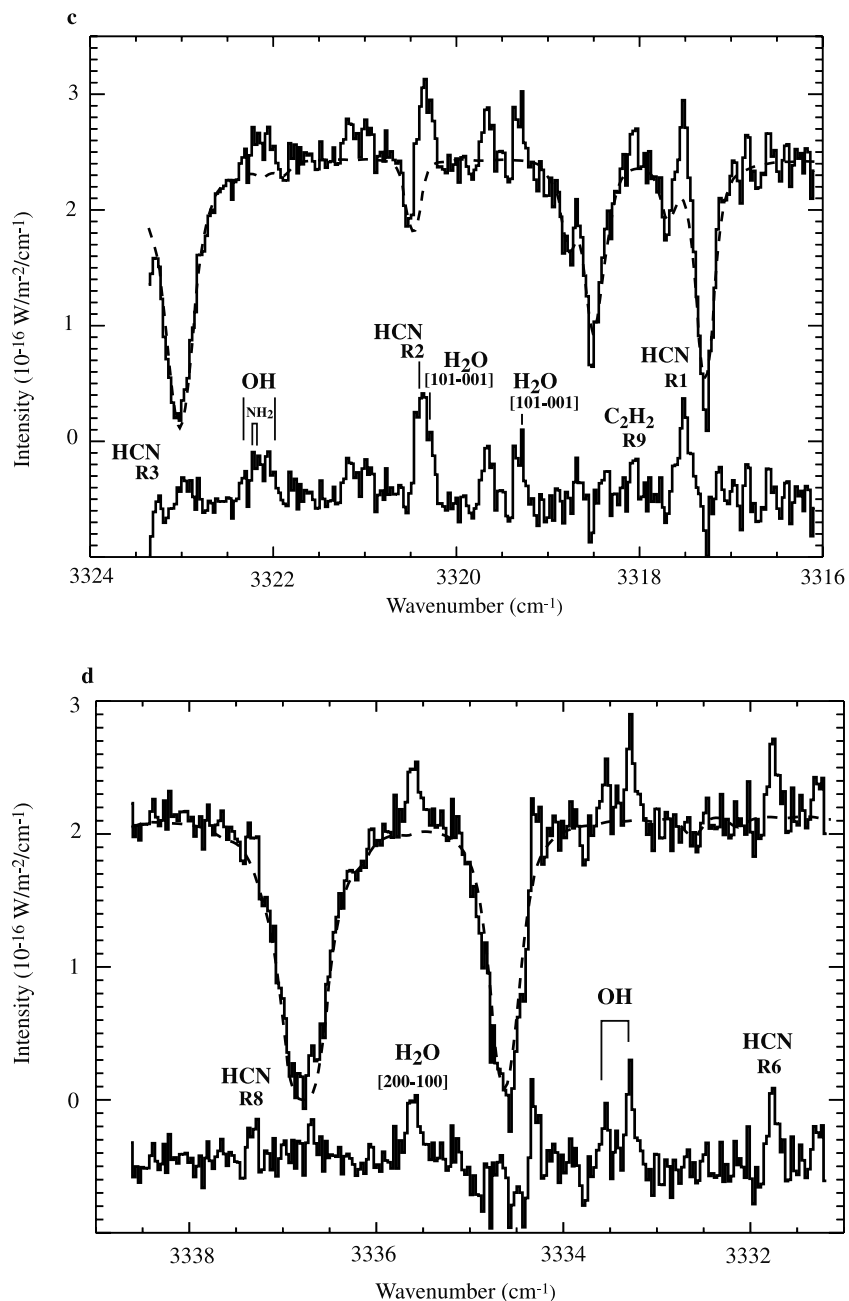


Figure 1. (continued)

[14] A reliable rotational temperature could be retrieved only for the nucleus-centered extract owing to low signal-to-noise ratios in regions offset from the nucleus. Using the intensity within a  $1'' \times 1''$  box, we determined the rotational temperature for a region centered on the nucleus to be  $83 \pm 9$  K (Table 1, Figure 2). This retrieved temperature characterizes the population of the (001) vibrational level. We assume this temperature also reflects the rotational temperature of the (000) ground level, since a fluorescent event only changes  $J$  by  $\pm 1$  and many rotational levels are sampled [Magee-Sauer *et al.*, 1999]. The eight ro-vibrational lines stem from excited levels  $J' = 1, 2, 4, 5, 7, 9$  which together contain  $\sim 58\%$  of the entire population in the 001 vibrational level; their combined intensities represent  $\sim 42\%$  of the integrated  $\nu_3$  vibrational band emission.

[15] Our retrieved nucleus-centered temperature is consistent with that measured by *Lis et al.* [1997] for HCN (75K) on March 22.5, and also with temperatures they retrieved for CO ( $73 \pm 6$ ) K and CH<sub>3</sub>OH ( $69 \pm 10$ ) on March 24.5. Their measurements were made at millimeter wavelengths where beam sizes are much larger (for CSO, FWHM  $\sim 25$  arc-seconds at 1 mm). Using the Plateau-de-Bure interferometer (four 15-m apertures used in the single-dish mode near 241.8GHz, FWHM  $\sim 21$  arc-seconds), *Biver et al.* [1999a] retrieved  $71 \pm 6$  K for CH<sub>3</sub>OH on March 24.1. The apparent agreement among the infrared and millimeter measurements may be somewhat fortuitous, owing to their widely different spatial scales. Outflowing gas is expected to cool adiabatically near the nucleus, then transition to photolytic heating in the intermediate coma, with a temper-

**Table 2.** Critical Distance ( $R_c$ )<sup>a</sup>

Line	$\nu_o$ , $\text{cm}^{-1}$	$N_{\text{crit}}^b$ $10^{15} \text{ cm}^{-2}$	$R_c^c$ m
P2	3305.71	9.05	509
P3	3302.72	7.21	639
P5	3296.65	7.39	623
P6	3293.59	8.82	523
R1	3317.50	8.07	571
R3	3323.27	5.44	847
R6	3331.76	7.65	603
R8	3337.31	1.47	314

<sup>a</sup> Calculation for  $r_h = 1.06 \text{ AU}$ ,  $Q_{\text{total}}(\text{HCN}) = 4.5 \times 10^{26} \text{ molecules s}^{-1}$ ,  $T_{\text{rot}} = 83 \text{ K}$ .

<sup>b</sup> Critical column density for HCN where optical depth  $\tau = 1$ .

<sup>c</sup> Distance from the nucleus at which the optical depth of a given line of HCN reaches unity at line center ( $\tau = 1$ ) along a radius vector from the Sun to  $R_c$ .

ature minimum occurring between the two regions. Lacking detailed information on the true temperature profile, we therefore adopt a uniform rotational temperature of 83 K in our calculations, at each position along the slit.

#### 4.2. Spatial Distribution

[16] The spatial profile (column density) for a species released solely and uniformly at the nucleus, and expanding outward with constant velocity, should show  $\rho^{-1}$  distribution ( $\rho =$  projected distance from the nucleus). A species having a distributed contribution (e.g. CO, OCS) will fall off more slowly than  $\rho^{-1}$  [Dello Russo et al., 1998; DiSanti et al., 2001]. However, properties of the comet (e.g. outflow asymmetries) and observing conditions (primarily atmospheric seeing, and tracking errors) cause deviations from  $\rho^{-1}$  near the nucleus even in the absence of a distributed source [Dello Russo et al., 2000]. For this reason, we compare spatial profiles of HCN and dust (taken from the same spectrum) since seeing and drift will affect each in the same manner.

[17] A spatial profile is obtained for an individual emission line by summing over its spectral extent in a processed cometary frame. The resulting “strip” includes cometary line emission, dust continuum, and uncanceled sky (if any). We isolated the cometary molecular line emission by subtracting another strip that included only continuum; corrections were applied when the atmospheric transmittance and/or residual background levels differed for the two strips. More detailed descriptions of this process are given by Dello Russo et al. [1998, 2000], Magee-Sauer et al. [1999], and DiSanti et al. [2001].

[18] The eight ro-vibrational lines (R2 line excluded) sampled on UT March 24.4 were summed and their spatial profile was compared with the profile of the (normalized) dust continuum emission (Figure 3). The spatial profiles were examined to determine whether the distribution of HCN was characteristic of release at the nucleus alone or if release from a distributed source was also required. We found the HCN profile to be approximately east-west symmetric at all positions about the nucleus, while the continuum profiles reveal a slight asymmetry (Figure 3).

#### 4.3. Production Rate

[19] An effective “spherical” production rate ( $Q$ , molecules  $\text{sec}^{-1}$ ) may be derived from the intensity measured at a specific location, using the (idealized, but useful) assumption of uniform spherical outflow from the nucleus. A spherical production rate is obtained from

$$Q = \frac{4\pi\Delta^2 F}{(hc\nu)g_{1\tau_1}f(x)\beta},$$

where  $F$  is the measured partial band emission flux ( $\text{W m}^{-2}$ ) at the top of the atmosphere,  $f(x)$  is the fraction of the total coma burden (of HCN) contained within the sampled region

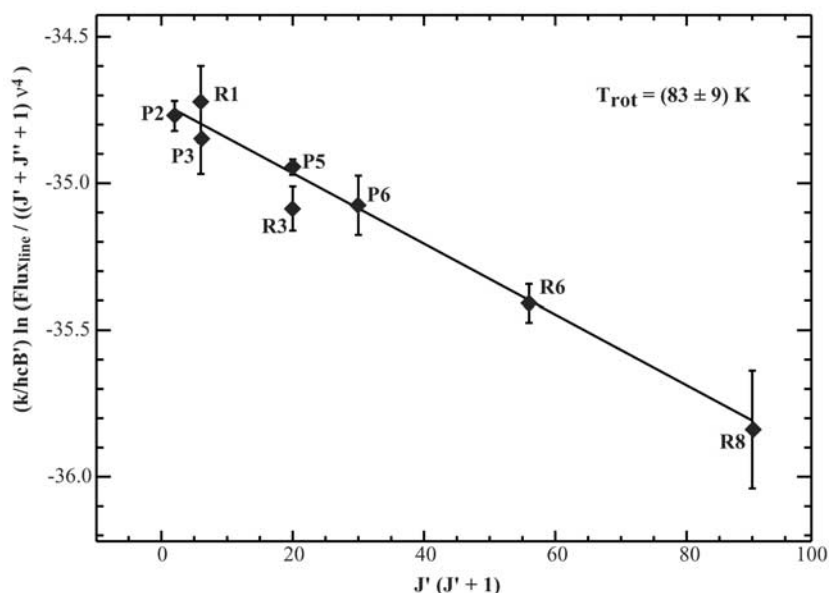


**Figure 2.** Rotational temperature analysis for 8 ro-vibrational lines of HCN on UT 1996 March 24.4. Line intensities are extracted from a  $1'' \times 1''$  box centered on the nucleus. The retrieved rotational temperature ( $T_{\text{rot}}$ ) was  $83 \pm 9 \text{ K}$  for the nuclear centered extracts.

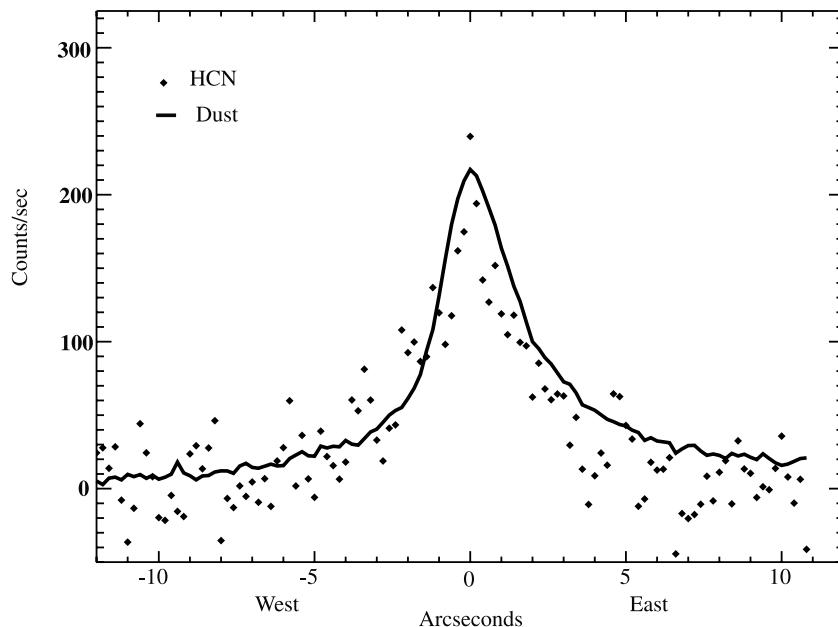


**Figure 3.** Spatial profile of HCN and dust for Comet Hyakutake UT 1996 March 24.4. The HCN profile (points) is east-west symmetric about its peak emission at all positions offset from the nucleus. The continuum profile (solid line) reveals significant asymmetry, being more extended toward the east. The dust profile is normalized to the mean of three HCN pixels centered on the nucleus.

[Hoban *et al.*, 1991],  $g_1$  is the band fluorescence efficiency ( $3.88 \times 10^{-4} \text{ s}^{-1}$  at 1 AU heliocentric distance),  $\beta$  is the fraction of the band intensity contained within the measured lines,  $\tau_1$  is the lifetime of the molecule (also at 1 AU), and  $hc\nu$  is the energy per photon (J). We adopt an outflow velocity ( $v$ ) of 0.8 km/s, in agreement with millimeter measurements near 1 AU preperihelion [Biver *et al.*, 1999a]. Since our projected distances are much smaller than the scale length ( $v\tau$ ) of the molecule,  $f(x)$  varies approximately as  $\tau^{-1}$ , making our retrieved production rates nearly independent of the specific value for the lifetime. We also note that  $\beta$  is not highly dependent on rotational temperature since we sample so many ro-vibrational lines.  $\beta$  increases by only  $\sim 3\%$  if we adopt a rotational temperature of 70K instead of 83K.

[20] We calculate the spherical production rate of the volatile as a function of distance from the nucleus (Figure 4a), and we obtain a symmetric production rate from the east-west mean at each offset distance (Figure 4b). The nucleus-centered extract is invariably low due to slit losses (primarily caused by seeing), but off-nucleus extracts of the symmetric Q are less affected by slit losses and quickly reach a terminal value (unless a distributed source is also present [DiSanti *et al.*, 2001]). The global production rate is defined as the weighted average of the spherical production rate in regions where measurements are less sensitive to slit losses and the apparent spherical production rates have reached the terminal value (for further discussion, see Magee-Sauer *et al.* [1999] and Dello Russo *et al.* [1998, 2000]). We obtain a global HCN production rate of  $(4.50 \pm 0.81) \times 10^{26} \text{ molecules s}^{-1}$ .

[21] Our group measured the water production rate in Hyakutake on the same night by observing five separate emission lines of  $\text{H}_2\text{O}$  in three vibrational hot bands using

CSHELL [Mumma *et al.*, 1996b; Dello Russo *et al.*, 2002]. The revised global production rate measured for  $\text{H}_2\text{O}$  was  $(2.54 \pm 0.25) \times 10^{29} \text{ molecules s}^{-1}$  [Dello Russo *et al.*, 2002], in good agreement with independent measurements on or near the same date based on  $\text{O}(^1\text{D})$  ( $2.77 \times 10^{29}$  [Hicks and Fink, 1997]) and on radio OH (a range of  $(2.5 \pm 0.5)$  to  $(3.3 \pm 1.1) \times 10^{29}$  for several inversion and quenching models [Gérard *et al.*, 1998]). The water production rate derived from H 121.6 nm on UT March 23 is somewhat smaller ( $1.8 \times 10^{29}$  [Bertaux *et al.*, 1998]), but this represents the mean production over the preceding ten days. An outburst occurred on UT March 21.4, and this could be responsible for the higher production rates measured on UT March 24 [Desvoivres *et al.*, 2000, and references therein]. Our absolute production rates correspond to a relative HCN/ $\text{H}_2\text{O}$  abundance of  $(0.18 \pm 0.04)\%$  on UT March 24.5.

## 5. Discussion

### 5.1. Rotational Temperature and Spatial Distribution

[22] We report the rotational temperature and production rate for HCN in comet Hyakutake on 1996 UT Mar 24.4, based on the measurement of 8 ro-vibrational lines (P2, P3, P5, P6, R1, R3, R6, R8). The rotational distribution is characterized by a single temperature, supporting a collisionally dominated region (Figure 2). The scatter among individual line intensities demonstrates the importance of including many ro-vibrational lines when determining the rotational temperature and ultimately the production rate.

[23] In comet Hale-Bopp, rotational temperatures for HCN and CO increased with distance from the nucleus due to photolytic heating of the coma [Magee-Sauer *et al.*,

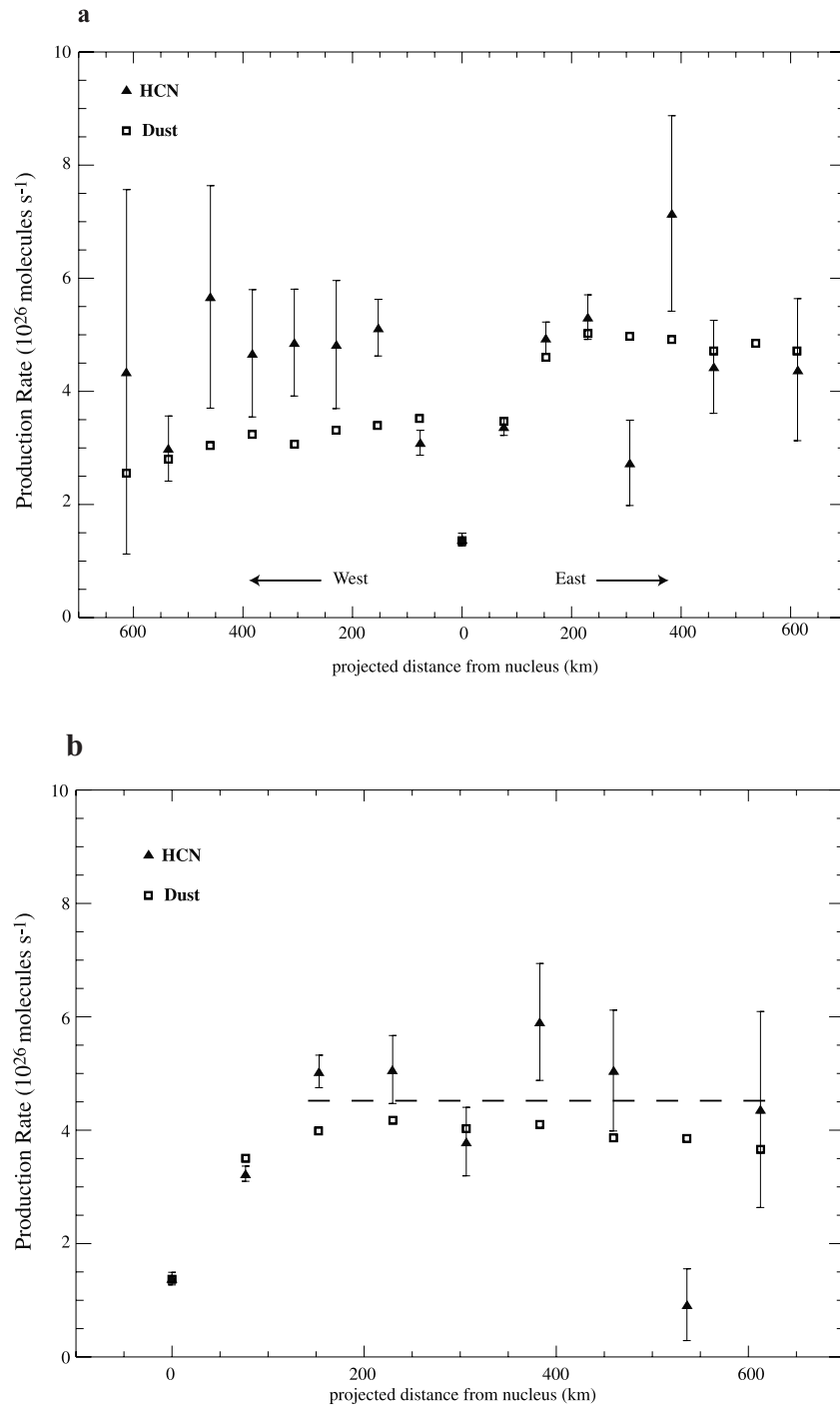


**Figure 4.** Retrieved production rates for HCN in Comet Hyakutake on UT 1996 March 24.4. (a) Spherical production rates for HCN (triangles) and dust (open squares) derived from the flux contained within a  $1'' \times 1''$  box. The box was stepped east and west of the nucleus at  $1''$  step intervals out to a distance of 8 arcseconds. Comparison of east and west extracts reveals no significant asymmetry in HCN. The spherical production rate for dust was scaled to the nucleus-centered production rate of HCN. A strong asymmetry favoring the sunward (east) direction is seen. (b) Symmetrized production rates for HCN (triangles) and dust (open squares), derived from a weighted average of east-west production rates. The global production rate derived was  $(4.52 \pm 0.81) \times 10^{26}$  molecules  $s^{-1}$  (dashed line).

1999; DiSanti *et al.*, 1999, 2001]. For HCN,  $T_{\text{rot}}$  was  $95 \pm 6$  K in the nucleus-centered extract, rising to  $\sim 120 \pm 14$  K at 2500 km offset from the nucleus (it was stable thereafter). It is not clear whether the increase seen in Hale-Bopp would

apply to Hyakutake. Owing to the much smaller geocentric distance (0.10 vs. 1.75 AU), the 30-arc-second slit sampled a much smaller region in Hyakutake ( $\pm 1100$  km about the nucleus), and we quantified HCN over only about half that

range or  $\sim\pm 600$  km about the nucleus. The nucleus-centered box ( $1'' \times 1''$ ) alone subtended  $\pm 637$  km about the nucleus in Hale-Bopp, but only  $\pm 37$  km in Hyakutake.

[24] The spatial profile of HCN in Hyakutake is consistent with that of a parent volatile; no significant contribution from a distributed source is required within  $\sim 600$  km of the nucleus (Figure 4b). This agrees with our results for comet Hale-Bopp on several dates [Magee-Sauer et al., 1999]. In neither Hyakutake nor Hale-Bopp do we see evidence for the release of significant additional HCN in the inner coma.

[25] Single-field millimeter images of HCN in comet Hale-Bopp also found no significant production in the inner coma (largest radial beam size  $\sim 20,000$  km) [Snyder et al., 2001]. However, Wright et al. [1998] analyzed the same data set using interferometric images combined with single-dish data to detect HCN out to a radial distance of  $\sim 50,000$  km, and they found evidence for excess HCN at larger radii (10,000–30,000 km).

## 5.2. Production Rate

[26] Our measured production rate for HCN in Hyakutake agrees with millimeter measurements made on the same night,  $(5.42 \pm 0.40) \times 10^{26}$  molecules  $s^{-1}$  (UT Mar 24 [Lovell, 1999]). However, our production rate is higher by a factor of  $\sim 2$  than millimeter measurements on dates bracketing our observations ( $2.5 \times 10^{26}$  molecules  $s^{-1}$  on UT Mar 23.5, and  $2.2 \times 10^{26}$  molecules  $s^{-1}$  on UT Mar 25.5) [Lis et al., 1997]. Their HCN production rate was a factor of two larger ( $4.1 \times 10^{26}$ ) on UT March 20.5 – 22.5. This behavior is surprising, since other evidence supports enhanced activity through March 24 following the outburst of March 21.4 [Schleicher et al., 1998; Gérard et al., 1998; Desvoires et al., 2000]. A direct comparison of absolute and relative production rates obtained by different techniques can be misleading. Agreement of absolute production rates might be more coincidental than consistent when observing approach, beam sizes, and model complexity differ. Resolving this difference is an important problem to address, but it is beyond the scope of this paper. This difference could be due to model parameters, or to physical conditions in the coma that have not been considered.

[27] Independent infrared observations of HCN in comet Hyakutake were reported by Brooke et al. [1996]. Two ro-vibrational lines (P7, P8) were measured on 1996 UT Apr 8.2, however no rotational temperature was obtained. If the rotational temperature were 83K, these two lines would represent  $\sim 11\%$  of the total band flux (and they would sample  $\sim 20\%$  of the upper state population). Brooke et al. reported a production rate  $7 - 9 \times 10^{26}$  molecules  $s^{-1}$  for HCN, based on an adopted temperature of 100K and a nucleus-centered spectral extract. If HCN production were insolation limited ( $Q_{\text{HCN}}$  varies as  $r_h^{-2}$ ), their production rate on April 8.2 ( $r_h = 0.74$  AU) would suggest a production rate of  $3.4 - 4.4 \times 10^{26}$  molecules  $s^{-1}$  on March 24.4 ( $r_h = 1.06$  AU). Although nominally consistent with our value of  $4.50 \pm 0.81 \times 10^{26}$ , the agreement may be largely fortuitous since nucleus-centered extracts are known to underestimate the true production rate and the assumed rotational temperature may not be reliable. Brooke et al. did not measure  $\text{H}_2\text{O}$  directly. They adopted a range  $1.5 - 3 \times 10^{29}$  for water

production on UT April 8.2, based on preliminary results from other groups, yielding a mixing ratio ( $\text{HCN}/\text{H}_2\text{O}$ ) of  $0.2 - 0.6\%$ . This range is consistent with our value ( $0.18\% \pm 0.04\%$ ), but the limitations of their data set prevent a critical comparison.

## 5.3. Relative Abundance

[28] The abundance of HCN relative to  $\text{H}_2\text{O}$  was similar in comets Hyakutake and Lee [Mumma et al., 2001], but it was somewhat higher in comet Hale-Bopp (Table 1). This is true for the relative HCN abundance measured by both infrared and millimeter observers. Although the absolute production rate of HCN measured by our infrared measurements and those of millimeter measurements [Biver et al., 1999a, 1999b; Lis et al., 1997] are not in agreement, both groups do agree that the abundance of HCN in Hale-Bopp was about a factor of 2 higher than that measured in Hyakutake and most other comets. It should be noted that Hale-Bopp was a very dusty comet, perhaps hinting that the high relative abundance of HCN might be related to dust. Although no extended source in the inner coma has been found for HCN in comets observed to date, this does not rule out the existence of a short-lived polymer released directly from the nucleus as a source for HCN within our field of view.

## 5.4. Comparison With Circumstellar Gas Near Young Stars

[29] It is interesting to compare cometary abundances of HCN with those measured by ISO-SWS for warm gases toward massive young stellar objects (YSOs) [Bockelée-Morvan et al., 2000; Lahuis and van Dishoeck, 2000]. Since comets are an ultimate product of the chemical evolution from interstellar grains to planetary systems, their volatile inventories provide important insights into evolutionary processes [Irvine et al., 2000].

[30] Gas-phase abundances in YSOs require HCN to be present at a level of  $\sim 0.5\%$  in the ices if their evaporation is the sole source of the HCN observed by ISO-SWS [Lahuis and van Dishoeck, 2000]. Our results for HCN in Hale-Bopp (0.4%) are consistent with this abundance. If ices near those young stars were similar to those in Hale-Bopp, all HCN observed by ISO-SWS could be the result of direct evaporation from ices and that no HCN is required from high temperature gas-phase reactions in the hot core. However, the relative abundance of HCN in comets Hyakutake and Lee is somewhat lower, showing that some differences exist among precometary ices from the 5–40 AU nebular range. If some HCN can be released from grains or from polymers, these might contribute an additional source for HCN in hot cores or comets. We note that small dust grains were much more abundant in Hale-Bopp than in other comets [Schleicher et al., 1997; Hanner et al., 1999].

[31] Ices in Hale-Bopp show evidence of formation at temperatures near 25–30K [Crovisier et al., 1997; Meier et al., 1998a, 1998b], suggesting they are interstellar, or at least were formed in a cold region of the early solar nebula (perhaps near Neptune). However, if Hyakutake and Lee (rather than Hale-Bopp) are representative of interstellar ices, the HCN abundance observed by ISO cannot be due only to evaporation from grain mantles, but would require a

contribution from gas-phase reactions in the hot core. The difference in HCN abundance among Hale-Bopp, Hyakutake and Lee might indicate different chemistries within the 5–40 AU region of the nebula where these Oort cloud comets were presumably created.

[32] Observations of more Oort cloud and Kuiper belt comets are needed to clarify the possible taxonomic classes. Furthermore, more detailed modeling of HCN chemistry in hot cores and preplanetary disks is needed before we can relate HCN abundances in comets to those in hot cores with confidence.

## 6. Conclusion

[33] Comets are a key to understanding the origin and evolution of our solar system. The volatile chemistry (identity and abundance) is a fingerprint of the physical and chemical conditions under which they were formed. For this reason, it is central to understanding the evolution of interstellar material into planetary systems and then comets.

[34] Relative abundances of volatiles in comets are particularly important and will help clarify whether some comets inherited their ices directly from interstellar grains in the natal cloud or if some precometary ices were processed in the presolar nebula. When measuring abundances for volatile species, it is important that these measurements feature an internally consistent method for retrieving the respective production rates. Otherwise, the individual production rates are subject to systematic errors related to the measurement approach (beam size, etc.) or to the analysis procedure (model assumptions, etc.). Our HCN production rates are compared with water production rates that are obtained from direct measurements of H<sub>2</sub>O on the same day with the same instrument and analyzed with the same basic algorithms, using model parameters appropriate to water. This reduces substantially the systematic errors that can be introduced when different instruments and/or different models for reduction are used.

[35] Measurement of multiple species at essentially the same moment in time further reduces systematic errors. With the advent of cross-dispersed spectrometers on large aperture telescopes (e.g. NIRSPEC [McLean et al., 1998] on Keck 2), the efficiency of high-resolution infrared spectroscopy is greatly improved. With NIRSPEC, for example, nearly the entire  $\nu_3$  band of the HCN molecule is obtained in one grating setting. Other orders measured simultaneously in the same grating setting include spectral lines of other volatiles, e.g. H<sub>2</sub>O, C<sub>2</sub>H<sub>6</sub>, C<sub>2</sub>H<sub>2</sub>, CH<sub>3</sub>OH, NH<sub>3</sub>, etc. Thus, a wide variety of volatiles are measured efficiently and in a manner by which systematic errors are greatly reduced. This is particularly notable for molecules that have no permanent dipole moment and as a result can only be studied at infrared wavelengths. The enhanced sensitivity improves detection limits for less abundant chemical species (e.g., HDO, HNC), and enhances the extraction of cosmogenic indicators such as isotopic ratios and nuclear spin temperatures.

[36] Moreover, the greatly improved efficiency of instruments such as NIRSPEC permits measurements to be made on less active comets, thereby opening a much larger population to investigation. The compositional differences

and similarities revealed in comets will lead to a better understanding of the dominant processes during formation of the solar system.

[37] **Acknowledgments.** This work was supported by the National Science Foundation Research at Undergraduates Institution program under grant AST-009841 to K. Magee-Sauer and by Rowan University, by the NASA Planetary Astronomy Program under RTOP 344-32-30-07 (M.J. Mumma), NAG5-7905 (M.A. DiSanti), and by the NASA Planetary Atmospheres Program under NAG5-7753 and NAG-10795 (N. Dello Russo). We are grateful to the outstanding support from the staff of the NASA Infrared Telescope Facility. The University of Hawaii under contract to NASA operates the NASA IRTF.

## References

- Bertaux, J. L., J. Costa, E. Quémerais, R. Lallement, M. Berthé, E. Kyrölä, W. Schmidt, T. Summanen, T. Makinen, and C. Goukenleuque, Lyman-alpha observations of comet Hyakutake with SWAN on SOHO, *Planet. Space Sci.*, *46*, 555–568, 1998.
- Biver, N., et al., Spectroscopic monitoring of comet C/1996 B2 (Hyakutake) with the JCMT and IRAM radio telescopes, *Astron. J.*, *118*, 1850–1872, 1999a.
- Biver, N., et al., Long term evolution of the outgassing of comet Hale-Bopp (C/1995 O1) from radio observations, *Earth Moon Planets*, *78*, 5–11, 1999b.
- Bockelée-Morvan, D., et al., New molecules found in comet C/1995 O1 (Hale-Bopp): Investigating the link between cometary and interstellar material, *Astron. Astrophys.*, *353*, 1101–1114, 2000.
- Brooke, T. Y., A. T. Tokunaga, H. A. Weaver, G. Chin, and T. R. Geballe, A sensitive upper limit on the methane abundance in comet Levy (1990c), *Astrophys. J.*, *372*, L113–L116, 1991.
- Brooke, T. Y., A. T. Tokunaga, H. A. Weaver, J. Crovisier, D. Bockelée-Morvan, and D. Crisp, Detection of acetylene in the infrared spectrum of comet Hyakutake, *Nature*, *383*, 606–608, 1996.
- Crovisier, J., K. Leech, D. Bockelée-Morvan, T. Y. Brooke, M. S. Hanner, B. Altieri, H. U. Keller, and E. Lellouche, The spectrum of comet Hale-Bopp (C/1995 O1) observed with the Infrared Space Observatory at 2.9 astronomical units from the Sun, *Science*, *275*, 1904–1907, 1997.
- Dello Russo, N., M. A. DiSanti, M. J. Mumma, K. Magee-Sauer, and T. W. Rettig, Carbonyl sulfide in comets C/1996 B2 (Hyakutake) and C/1995 O1 (Hale-Bopp): Evidence for an extended source in Hale-Bopp, *Icarus*, *135*, 377–388, 1998.
- Dello Russo, N., M. J. Mumma, M. A. DiSanti, K. Magee-Sauer, R. Novak, and T. W. Rettig, Water production and release in comet C/1995 O1 (Hale-Bopp), *Icarus*, *143*, 324–337, 2000.
- Dello Russo, N., M. J. Mumma, M. A. DiSanti, K. Magee-Sauer, and R. Novak, Ethane production and release in comet C/1995 O1 Hale-Bopp, *Icarus*, *153*, 162–179, 2001.
- Dello Russo, N., M. J. Mumma, M. A. DiSanti, and K. Magee-Sauer, Production of ethane and water in comet C/1996 B2 Hyakutake, *J. Geophys. Res.*, *107*, 10.1029/2001JE001838, in press, 2002.
- Desvoivres, E., J. Klinger, A. C. Levasseur-Regourd, and G. H. Jones, Modeling the dynamics of cometary fragments: Application to comet C/1996 B2 Hyakutake, *Icarus*, *144*, 172–181, 2000.
- DiSanti, M. A., M. J. Mumma, J. H. Lacy, and P. Parmar, A possible detection of infrared emission from carbon monoxide in Comet Austin (1989c1), *Icarus*, *96*, 151–160, 1992a.
- DiSanti, M. A., M. J. Mumma, and J. H. Lacy, A sensitive upper limit to OCS in comet Austin (1989c1) from a search for  $\nu_3$  emission at 4.85  $\mu$ m, *Icarus*, *97*, 155–158, 1992b.
- DiSanti, M. A., M. J. Mumma, N. Dello Russo, K. Magee-Sauer, R. Novak, and T. W. Rettig, Identification of two sources for carbon monoxide in comet Hale-Bopp, *Nature*, *399*, 662–665, 1999.
- DiSanti, M. A., M. J. Mumma, N. Dello Russo, and K. Magee-Sauer, Carbon monoxide production and excitation in Comet C/1995 O1 (Hale-Bopp): Isolation of native and distributed CO sources, *Icarus*, *153*, 361–390, 2001.
- Gérard, E., J. Crovisier, P. Colom, N. Biver, D. Bockelée-Morvan, and H. Rauer, Observations of the OH radical in comet C/1996 B2 (Hyakutake) with the Nançay radio telescope, *Planet. Space Sci.*, *46*, 569–577, 1998.
- Greene, T. P., A. T. Tokunaga, D. W. Toomey, and J. S. Carr, CSHELL: A high spectral resolution 1–5 micron cryogenic echelle spectrograph for the IRTF, *Proc. SPIE Int. Soc. Opt. Eng.*, *1946*, 311, 1993.
- Hanner, M. S., R. D. Gehrz, D. E. Harker, T. L. Hayward, D. K. Lynch, C. C. Mason, R. W. Russell, D. M. Williams, D. H. Wooden, and C. E. Woodward, Thermal emission from the dust coma of comet Hale-Bopp

- and the composition of the silicate grains, *Earth Moon Planets*, 79, 247–264, 1999.
- Harmon, J. K., et al., Radar detection of the nucleus and coma of comet Hyakutake (C/1996 B2), *Science*, 278, 1921–1924, 1997.
- Herzberg, G., *Spectra of Diatomic Molecules*, p. 126, Van Nostrand Reinhold, New York, 1950.
- Hicks, M., and U. Fink, Spectrophotometry and the development of emissions for C/1996 B2 (comet Hyakutake), *Icarus*, 127, 307–318, 1997.
- Hoban, S., M. J. Mumma, D. C. Reuter, M. DiSanti, R. R. Joyce, and A. Storrs, A tentative identification of methanol as the progenitor of the 3.52  $\mu\text{m}$  feature in several comets, *Icarus*, 93, 122–134, 1991.
- Huebner, W. F., L. E. Snyder, and D. Buhl, HCN radio emission from comet Kohoutek (1973f), *Icarus*, 23, 580–585, 1974.
- Irvine, W. M., F. P. Schloerb, J. Crovisier, B. Fegley, and M. J. Mumma, Comets: A link between interstellar and nebular chemistry, in *Protostars and Planets IV*, edited by V. Manning, A. P. Boss, and S. S. Russell, pp. 1159–1200, Univ. of Ariz. Press, Tucson, 2000.
- Lahuis, F., and E. F. van Dishoeck, ISO-SWS spectroscopy of gas-phase  $\text{C}_2\text{H}_2$  and HCN toward massive young stellar objects, *Astron. Astrophys.*, 355, 699–712, 2000.
- Lis, D. C., J. Keene, K. Young, T. G. Phillips, D. Bockelée-Morvan, J. Crovisier, P. Schilke, P. F. Goldsmith, and E. A. Bergin, Spectroscopic observations of comet C1996 B2 (Hyakutake) with the Caltech Submillimeter Observatory, *Icarus*, 130, 355–372, 1997.
- Lovell, A. J., Millimeter-wave molecular mapping of comets Hyakutake and Hale-Bopp, Ph.D. thesis, Univ. of Mass., Amherst, 1999.
- Magee-Sauer, K., M. J. Mumma, M. A. DiSanti, N. Dello Russo, and T. Rettig, Infrared spectroscopy of the  $\nu_3$  band of hydrogen cyanide in comet C/1995 O1 Hale-Bopp, *Icarus*, 142, 498–508, 1999.
- McLean, I. S., et al., The design and development of NIRSPEC: A near-infrared echelle spectrograph for the Keck II telescope, in *Infrared Detector Arrays for Astronomy*, edited by A. M. Fowler, *Proc. SPIE Int. Soc. Opt. Eng.*, 3354, pp. 566–578, 1998.
- Meier, R., T. C. Owen, H. E. Matthews, D. C. Jewitt, D. Bockelée-Morvan, N. Biver, J. Crovisier, and D. Gautier, A determination of the HDO/ $\text{H}_2\text{O}$  ratio in comet C/1995 O1 (Hale-Bopp), *Science*, 279, 842–844, 1998a.
- Meier, R., T. C. Owen, D. C. Jewitt, H. E. Matthews, M. Senay, N. Biver, D. Bockelée-Morvan, J. Crovisier, and D. Gautier, Deuterium in comet C/1995 O1 (Hale-Bopp): Detection of DCN, *Science*, 279, 1707–1710, 1998b.
- Mumma, M. J., H. A. Weaver, H. P. Larson, M. Williams, and D. Davis, Detection of water vapor in Halley's comet, *Science*, 232, 1523–1528, 1986.
- Mumma, M. J., P. R. Weissman, and S. A. Stern, Comets and the origin of the solar system: Reading the Rosetta Stone, in *Protostars and Planets III*, edited by E. H. Levy and J. I. Lunine, pp. 1177–1252, Univ. of Ariz. Press, Tucson, 1993.
- Mumma, M. J., M. A. DiSanti, and X. Xie, *IAU Circ.* 6228, Int. Astron. Union, Paris, 1995a.
- Mumma, M. J., M. A. DiSanti, A. T. Tokunaga, and E. E. Roettger, Ground-based detection of water in comet Shoemaker-Levy 1992 XIX: Probing cometary parent molecules by hot-band fluorescence, *Bull. Am. Astron. Soc.*, 27, 1144, 1995b.
- Mumma, M. J., M. A. DiSanti, N. Dello Russo, D. X. Xie, M. Fomenkova, and K. Magee-Sauer, *IAU Circ.* 6366, Int. Astron. Union, Paris, 1996a.
- Mumma, M. J., M. A. DiSanti, N. Dello Russo, M. Fomenkova, K. Magee-Sauer, C. D. Kaminski, and D. X. Xie, Detection of abundant ethane and methane, along with carbon monoxide and water, in Comet C/1996 B2 Hyakutake: Evidence for processed interstellar ice, *Science*, 272, 1310–1314, 1996b.
- Mumma, M. J., et al., A survey of organic volatile species in comet H1 (Lee) using NIRSPEC at the Keck Observatory, *Astrophys. J.*, 546, 1183–1193, 2001.
- Schleicher, D. G., S. M. Lederer, R. L. Millis, and T. L. Farnham, Photometric behavior of comet Hale-Bopp (C/1995 O1) before perihelion, *Science*, 275, 1913–1915, 1997.
- Schleicher, D. G., R. L. Millis, D. J. Osip, and S. M. Lederer, Activity and the rotation period of comet Hyakutake (1996 B2), *Icarus*, 131, 233–244, 1998.
- Schloerb, F. P., W. M. Kinzel, D. A. Swade, and W. M. Irvine, HCN production from comet Halley, *Astrophys. J.*, 310, L55–L60, 1986.
- Snyder, L. E., J. M. Veal, L. M. Woodney, M. C. H. Wright, P. Palmer, M. F. A'Hearn, Y.-J. Kuan, I. De Pater, and J. R. Forster, BIMA array photodissociation measurements of HCN and CS in Comet Hale-Bopp (C/1995 O1), *Astron. J.*, 121, 1147–1154, 2001.
- Tokunaga, A. T., D. W. Toomey, J. Carr, D. N. B. Hall, and H. W. Epps, Design for a 1- to 5- $\mu\text{m}$  cryogenic echelle spectrograph for the NASA IRTF, in *Instrumentation in Astronomy VII*, edited by D. Crawford, *Proc. SPIE Int. Soc. Opt. Eng.*, 1235, part 2, 131–143, 1990.
- Weaver, H. A., M. J. Mumma, H. P. Larson, and D. Davis, Post-perihelion observations of water in comet Halley, *Nature*, 324, 441–444, 1986.
- Weaver, H. A., T. Y. Brooke, G. Chin, S. J. Kim, D. Bockelée-Morvan, and J. K. Davies, Infrared spectroscopy of comet Hale-Bopp, *Earth Moon Planets*, 78, 71–80, 1999.
- Wright, M. C. H., et al., Mosaiced images and spectra of J = 1-0 HCN and  $\text{HCO}^+$  emission from Comet Hale-Bopp (1995 O1), *Astron. J.*, 116, 3018–3028, 1998.

---

M. DiSanti and N. Dello Russo, Department of Physics, Catholic University of America, Washington, DC 20064, USA.

K. Magee-Sauer, Department of Chemistry and Physics, Rowan University, Glassboro, NJ 08028, USA. (sauer@rowan.edu)

M. J. Mumma, Laboratory for Extraterrestrial Physics, NASA Goddard Space Flight Center, Code 690, Greenbelt, MD 20771, USA.